IOP Publishing Journal of Physics: Condensed Matter
J. Phys.: Condens. Matter **32** (2020) 494001 (7pp) https://doi.org/10.1088/1361-648X/abb0a5

Mechanical and dielectric response within and beyond the linear regime

Birte Riechers[1,3] **and Ranko Richert**[2]

[1] Glass and Time, IMFUFA, Department of Science and Environment, DK-4000 Roskilde University, Roskilde, Denmark
[2] School of Molecular Sciences, Arizona State University, Tempe, Arizona 85287, United States of America

E-mail: birteri@ruc.dk

Received 25 June 2020, revised 6 August 2020
Accepted for publication 19 August 2020
Published 10 September 2020

Abstract

In this work a comparison of dielectric and mechanical data is presented based on experiments within the linear response limit and beyond that limit. The linear dynamic and shear-mechanical response is discussed in terms of the molecular supercooled liquid tetramethyl-tetraphenyl-trisiloxane. As the dynamics measured by the two methods depict the same temperature-dependence, the underlying cause for the observed responses is assumed to be identical for both methods, namely structural relaxation. The comparison of dielectric and mechanical measurements under high excitation amplitudes reveals that this cannot be assumed for the nonlinear response: Mechanical experiments on metallic glasses suggest that involved energies are clearly beyond k_BT, with observed nonlinear effects based on the activation of microstructural plastic rearrangements. In contrast, nonlinear dielectric measurements on another molecular glass-former involve energies clearly below k_BT, so that nonlinear dielectric effects occur due to energy uptake from the electric field or entropy-based changes in the dynamics, but are very unlikely connected to the triggering of plastic rearrangements by the applied electric field.

Keywords: linear response, nonlinear response, dielectric spectroscopy, mechanical spectroscopy, compliance

(Some figures may appear in colour only in the online journal)

1. Introduction

The glassy state of matter is key to many technological applications, but also poses challenging questions regarding the fundamental sciences of structure and dynamics of these non-crystalline solids. In many cases, the supercooled liquid is the precursor to the glassy state, which can be achieved by cooling the liquid below the glass transition temperature T_g [1]. Alternatively, the transition into the glassy state can also be driven by pressure elevation, by solvent evaporation, or by physical vapor deposition onto substrates held at $T < T_g$ [2, 3]. Experimentally, the glass transition appears as a kinetic effect, and the value of T_g is thus defined somewhat arbitrarily by the temperature at which the average structural relaxation time is $\tau_\alpha(T_g) = \tau_g = 100$ s. While this criterion based on τ_g might appear straightforward, such a definition of T_g does not specify how to measure the (primary or α-) relaxation time. In any case, the dynamics of the equilibrium liquid just above T_g will impact the properties of the non-equilibrium glassy state obtained by lowering the temperature at a specific cooling rate.

Many different experimental techniques are capable of observing signatures of the primary structural relaxation: optical scattering techniques [4], dielectric spectroscopy [5], mechanical measurements [6], nuclear magnetic resonance techniques [7], as well as calorimetry [8], to name a few. Common to these techniques is the observation of a super-Arrhenius temperature dependence for $\tau_\alpha(T)$, often following the empirical Vogel–Fulcher–Tammann (VFT) relation [9, 10, 11]:

[3] Author to whom any correspondence should be addressed.

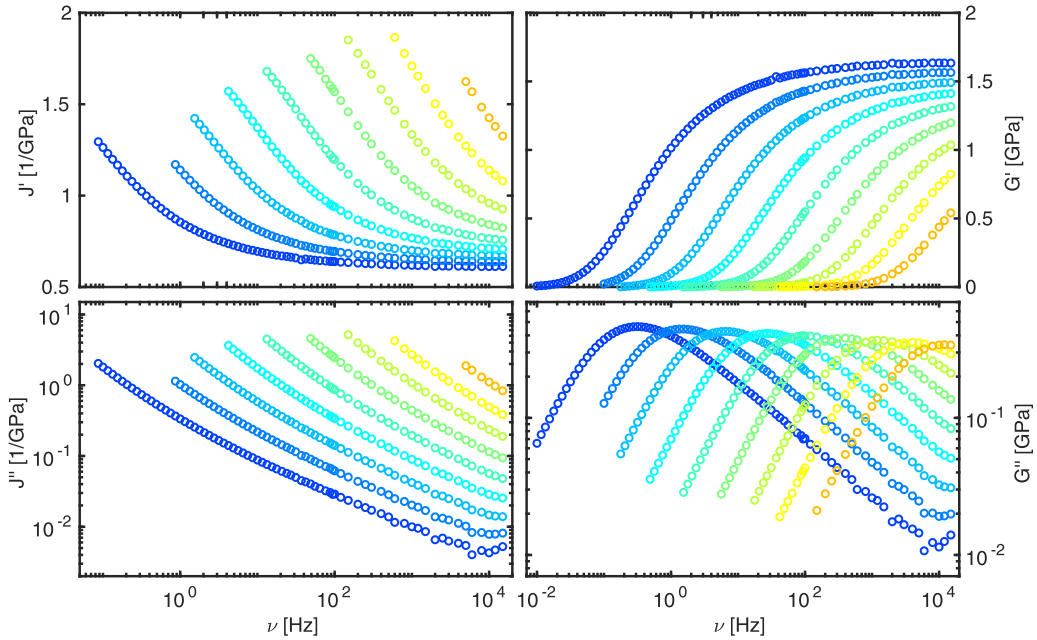

Figure 1. Linear storage and loss contribution of shear compliance $J(\omega)$ and shear modulus $G(\omega)$ for tetramethyl-tetraphenyl-trisiloxane at temperatures ranging from $T = 215$ to 232 K in 2 K steps measured in parallel-plate geometry. Data from reference [16].

	Shear-mechanical	Dielectric
Compliance (retardation)	$\gamma = J\sigma$	$D = \varepsilon\varepsilon_0 E$
Modulus (relaxation)	$\sigma = G\gamma$	$\varepsilon_0 E = MD$

$$\log_{10}\left(\tau_\alpha/s\right) = A + \frac{B}{T - T_0}. \tag{1}$$

When different techniques are employed to measure the temperature dependent relaxation behavior for the same material, it is often found that the resulting $\tau_\alpha(T)$ curves all follow the VFT pattern. Moreover, very similar activation parameters B and divergence temperatures T_0 can be obtained from different techniques, whereas the offset A is more technique specific. Despite the similarities in the activation behavior, different techniques probe different correlation functions which are bound to display different values for τ_α at a given temperature and pressure. To date, there is no straightforward method of predicting the relaxation function for one technique from that of another.

The typical approach to characterizing the relaxation dynamics of a material is to perturb the system, i.e., to alter the value of an external variable such that the system is forced to approach the new equilibrium state by a relaxation or retardation process. It is usually desired to keep the magnitude of the perturbation sufficiently small so that properties such as the relaxation times are not altered considerably by virtue of the perturbation. This represents the limit of linear response [12], i.e., the regime in which the response function does not depend on the magnitude of the perturbation. The majority of relaxation experiments fall into this category.

In recent years, relaxation behavior outside the linear response regime has gathered significant interest. When perturbations become large enough in magnitude, the technique applied not only probes the sample but also modifies its properties. For instance, a low amplitude mechanical shear experiment follows Hooke's law of linear response, but high shear rates may lead to shear thinning or even sample failure. In this regime, analysis tools such as Boltzmann superposition principle, Kramers–Kronig relations, and the fluctuation dissipation theorem no longer apply, thereby complicating the comparison of results from different techniques even further. Forces that drive the system beyond the regime of linear response remove the system away from equilibrium, and one approach to characterizing a non-equilibrium state is based on the concept of the fictive temperature, T_f [13]. For a non-equilibrium state X_noneq at temperature T, this variable T_f is generally defined as the temperature that produces the same state X_equil if the system were in equilibrium, $X_\mathrm{noneq}(T) = X_\mathrm{equil}(T_\mathrm{f})$.

This work focuses on the comparison of shear mechanical and dielectric relaxation, two widely applied techniques used to characterize the dynamics of glass forming materials. A main point to be stressed is that understanding the relation between mechanical and dielectric responses in the linear response is no guarantee for an analogous relation to apply for the two nonlinear counterparts.

2. Mechanical and dielectric response in the linear limit

In the linear response regime, the stress-strain relation is characterized by Hooke's law. In its generalized form it reads

$$\sigma_{ij} = c_{ijkl} \cdot \gamma_{kl}, \tag{2}$$

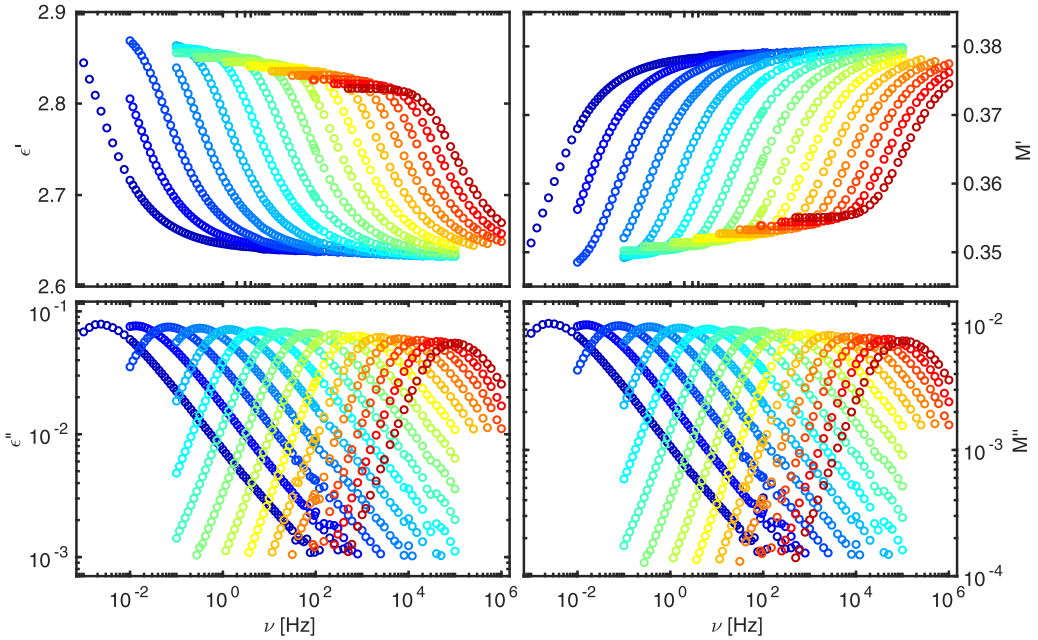

Figure 2. Linear storage and loss contribution of dielectric permittivity $\varepsilon(\omega)$ and dielectric modulus $M(\omega)$ for tetramethyl-tetraphenyl-trisiloxane at temperatures ranging from $T = 211$ to 240 K. Data from reference [16].

with the stress tensor, σ_{ij}, the strain tensor, γ_{kl}, and the elasticity tensor, c_{ijkl}, which holds 81 entries, but is significantly reduced due to symmetry relations. Thus, for isotropic materials, the mechanical response to an arbitrary excitation can be characterized by a pair of two moduli from the following set of quantities: bulk modulus, shear modulus, Young's modulus, Poisson's ratio, and longitudinal modulus.

One of the most fundamental moduli is the shear modulus, G, which characterizes a volume preserving deformation, measuring the elastic resistance to shape-change. In case of a shear deformation, the linear stress-strain-relation can be expressed as

$$\sigma = G \cdot \gamma, \tag{3}$$

where the strain represents the exciting force that relates to the stress response σ in the manner of a conventional relaxation experiment. The conjugate of the shear modulus is experimentally addressed by a stress-driven retardation experiment, and referred to as complex shear compliance, $J(\omega) = 1/G(\omega)$, or

$$J'(\omega) - i \cdot J''(\omega) = \left(G'(\omega) + i \cdot G''(\omega)\right)^{-1}. \tag{4}$$

A number of shear-mechanical experimental techniques involving parallel plate, torsional, or coaxial cylinder geometries allow for a characterization of $G(\omega)$ and $J(\omega)$ as complex, dynamic functions. Limitations are typically found as restrictions in the available frequency range due to setup-specific resonances that define the upper frequency limit or in the measurable viscosity range that is restricted by the setup's internal stiffness.

An example of dynamic, shear-mechanical data linearly measured by a parallel plate technique that was developed by Olsen and Christensen [14, 15] is given in figure 1. This technique is capable of measurements of deeply supercooled liquids at frequencies from Millihertz to 10 Kilohertz. The storage and loss contribution of both shear compliance and shear modulus are shown for several temperatures very close to and above the glass transition temperature T_g for tetramethyl-tetraphenyl-trisiloxane.

The peak of the loss modulus data in figure 1(d) and its corresponding step in the storage modulus G' (figure 1(c)) reflect the transition from glassy to liquid-like behavior. Normalizing the loss modulus to the amplitude and position of the loss peak results in a collapse of the spectra, indicating that the principle of time-temperature-superposition is obeyed within the investigated temperature range. The low-frequency flank of the loss spectra follows a powerlaw with exponent one, reflecting Newtonian behavior [17]. In comparison to modulus data, the compliance is more sensitive to the material's shear-flow [17]. The loss contribution shown in figure 1(b) can be described as a sum of a viscosity-related term, which is equal to the inverse product of viscosity and angular frequency, and the relaxational term. By subtraction of this viscosity-related term from the overall loss compliance, the timescale connected to the shear compliance can be determined from the maximum of the resulting loss difference.

The constitutive relations representing the retardation and relaxation function pairs for linear dielectric and shear-mechanical experiments read with the permittivity of vacuum ε_0, the dielectric displacement D, and the electric field E. Thus, following the same principle as in the shear-mechanical case, the dielectric permittivity equals the conjugated dielectric modulus [18], $\varepsilon(\omega) = 1/M(\omega)$, or

$$\varepsilon'(\omega) - i \cdot \varepsilon''(\omega) = \left(M'(\omega) + i \cdot M''(\omega)\right)^{-1}. \tag{5}$$

In case of a dielectric retardation experiment, the complex dielectric permittivity $\varepsilon(\omega)$ characterizes the sample response. The dielectric loss permittivity and modulus are plotted in

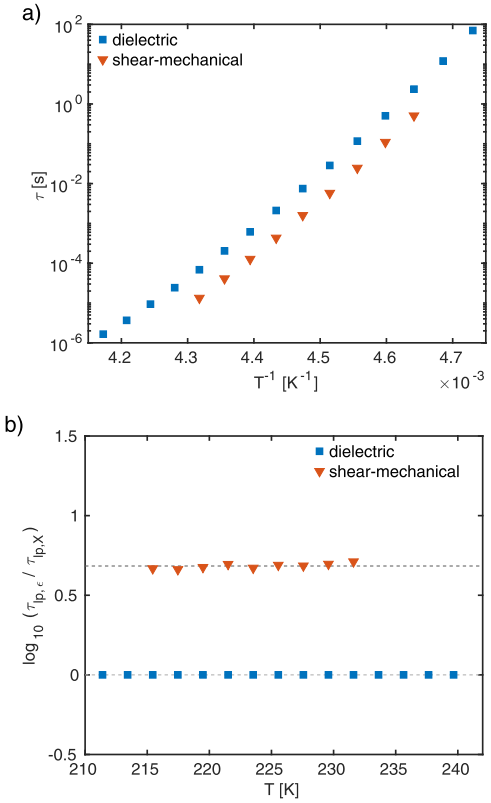

Figure 3. (a) Timescales of structural relaxation deduced from shear-mechanical loss modulus $G''(\omega)$ and dielectric loss permittivity $\varepsilon''(\omega)$ for tetramethyl-tetraphenyl-trisiloxane as a function of temperature based on data from [16]. (b) Timescale index as a function of temperature given by the logarithmic distance between the timescale of a response function X, i.e. shear or dielectric response, and the timescale of the dielectric response.

figures 2(b) and (d) for tetramethyl-tetraphenyl-trisiloxane for the temperature and frequency ranges of the glass transition.

Both representations exhibit a maximum in the loss spectrum, but comparisons of dielectric and shear-mechanical spectral shapes should be made with caution. Loss spectra of compliance and its conjugate modulus will generally differ in their shape, but a comparison of spectra in either the modulus or the compliance representations of different linear response functions may seem straightforward. However, the shape of $M''(\omega)$ is governed by the field-field correlation function and may thus contain electronic and conductivity contributions that are not directly associated with the primary structural relaxation [19]. Therefore, even though $M''(\omega)$ and $G''(\omega)$ are both moduli, their spectra should generally not be expected to match.

In a comparison of timescales the modulus and compliance representation of dielectric data do not hold identical temperature-dependence. As the loss modulus is connected to the loss permittivity as $M''(\omega) = \varepsilon''(\omega)/|\varepsilon(\omega)|^2$ and with $\varepsilon(\omega)$ being a monotonously decreasing function of frequency, it depends strongly on the relaxation strength of the material how intensely the relaxation timescales of $\varepsilon(\omega)$ and $M(\omega)$ differ. This is reflected in the relation $\tau_\varepsilon/\tau_M = \varepsilon_s/\varepsilon_\infty$ [20], where τ_ε and τ_M are the respective linear averages of the compliance and modulus relaxation times, and the ε_s and ε_∞ are the static and high frequency limits of permittivity, with $\varepsilon_s - \varepsilon_\infty$ being the relaxation strength that depends on temperature.

With the above reasoning on the timescale of the dielectric modulus and the uncertainty of the timescale for the relaxational part of shear compliance due to the necessary subtraction of the viscosity term, figure 3 is restricted to a comparison of the dynamics of the shear modulus and the dielectric permittivity. The dynamics for both response functions show a strong resemblance that can be captured by a fit to the VFT equation (1). The timescale index, which is the logarithmic distance of the relaxation time determined from the shear-mechanical data and the dielectric timescale, visualizes that shear-mechanical and dielectric response share the same temperature-dependence, indicating that both linear response functions are related to the same underlying process. This coupling between separate linear response functions seems to be a general feature for supercooled liquids with a pure primary relaxation contribution [16, 21, 22].

3. Nonlinear dielectric and mechanical response

The nonlinear response regime is characterized by an excitation-dependent compliance, with the degree of nonlinearity becoming more pronounced with increasing amplitude of exciting force. Nonlinear effects can appear as an increase or decrease in the compliance's steady state value, modification of its dynamics and also the appearance of higher harmonic contributions [23].

To give a general description of the relation between an exciting force F and its nonlinear response R, a power series can be utilized that reflects the steady state ($t \to \infty$) in the static limit ($\omega \to 0$) for a generalized compliance χ:

$$R = \chi F + \chi^{(2)}F^2 + \chi^{(3)}F^3 + \chi^{(4)}F^4 + \chi^{(5)}F^5 + \ldots. \quad (6)$$

The function of the exciting force can have various forms, such as a high magnitude bias or a high amplitude harmonic oscillation in shear strain [24, 25], electric [26, 27] or magnetic field [28]. The following description of nonlinear shear and dielectric experiments focuses on harmonically exciting forces $F(t) = F_0 \cos(\omega_0 t)$ for which the generalized response is regarded as symmetric, i.e., $R(F) = -R(-F)$, so that even terms of the power series become negligible.

Experimental data of a mechanical single cantilever bending experiment on the metallic glass $Pd_{40}Ni_{40}P_{20}$ are depicted in figure 4. These data are based on two different amplitudes of the applied harmonic shear stress. One is within the linear limit ($\sigma_0 = 10$ MPa) resulting in a shear strain with a measurable Fourier-contribution at the exciting frequency only. The higher stress amplitude ($\sigma_0 = 54$ MPa) yields a response connected to the early nonlinear regime as the strain response contains signal at higher order frequencies ($3\nu_0$, $5\nu_0$) as well, while the overall strain response is still mediocre compared to creep measurements of metallic glasses under bias stresses of comparable magnitude [29]. Further indications for nonlinear behavior are found as the compliance value that is identified as the quotient of shear strain and stress at the excitation frequency ν_0 and which is 10% higher than the one deduced from

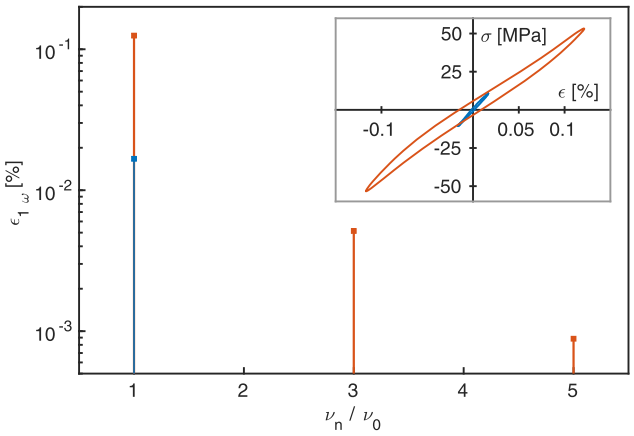

Figure 4. Strain contributions as mechanical response to harmonic stress excitation at a frequency of $\nu_0 = 1$ Hz at $\sigma_0 = 10$ MPa and $\sigma_0 = 54$ MPa stress amplitudes from a single cantilever bending experiment on $Pd_{40}Ni_{40}P_{20}$ at 565 K ($T_g = 575$ K). Note that higher harmonics are not resolved for the lower stress amplitude case. Inset: corresponding Lissajous representation for measurements with $\sigma_0 = 10$ MPa (blue) and $\sigma_0 = 54$ MPa (red).

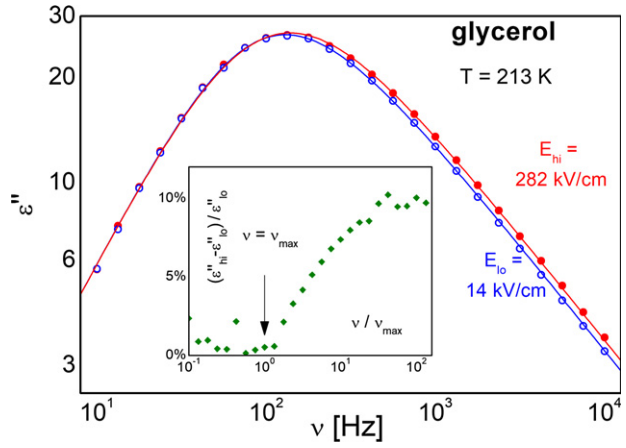

Figure 5. Loss contribution of dielectric permittivity, $\varepsilon''(\omega)$, of glycerol measured at two different amplitudes of an harmonic electric field, E_0, as a function of frequency [26]. The observed dielectric effect reflects an energy uptake from the electric field resulting in a shift of the high-frequency part of the spectrum towards higher frequencies. The inset displays the relative field induced change, $\left(\varepsilon''_{hi} - \varepsilon''_{lo}\right)/\varepsilon''_{lo}$, to emphasize the different effects for $\nu < \nu_{max}$ and $\nu > \nu_{max}$, with ν_{max} being the peak loss frequency. Adapted figure with permission from [26], Copyright (2006) by the American Physical Society.

the linear experiment, as well as the Lissajous representation (figure 4, inset) which is clearly distorted under excitation with the higher stress amplitude.

The increase in compliance resulting from nonlinear effects, reflecting a softening of the material under mechanical load, can be interpreted in terms of an excess fictive temperature ($T_f > T$) of the mechanically probed material, and is also referred to as mechanical softening, with the fictive temperature, T_f, defined as the temperature at which the equilibrated system has the present time constant τ [13]. Similar observations are made for many other materials [30] and in case of molecular dynamic simulations that report a strain-induced glass transition [31]. The cause of this effect is discussed as the mechanically induced activation of localized plastic events, which are cooperative rearranging regions [32] of local, plastic shear deformation surrounded by an elastically deformed strain field described by Eshelby analysis [33, 34], also referred to as shear transformation zones (STZ) [35, 36].

In case of dielectric experiments, multiple nonlinear effects are known, such as dielectric saturation [37–39], the so-called 'chemical effect' connected to the field-dependence of the Kirkwood-correlation factor g_K [39, 40], the electro-rheological effect, which is connected to field-induced changes in entropy, and energy absorption from the electrical field [23].

Experimental dielectric data is shown in figure 5 for the molecular glass-former glycerol [26]. The plot shows the loss contribution of dielectric permittivity based on a harmonic excitation amplitude within the linear limit at electric fields of $E_0 = 14$ kV cm^{-1}, and based on $E_0 = 282$ kV cm^{-1} yielding a nonlinear response for numerous frequencies covering the relaxation mode spectrum. One feature capturing the nonlinearity of the material's response is the excess in $\varepsilon''(\omega)$ under high field amplitude compared to the linear dielectric loss above the peak frequency. It can be interpreted in terms of a shift of that part of the spectrum towards higher frequencies, reflecting a field-induced state of elevated fictive temperature ($T_f > T$). Interestingly, applying a bias electric field instead of a high amplitude harmonic field results in the opposite effect. Here, the field-induced relative changes in the dielectric loss for all frequencies of the relaxation mode spectrum amount to a steady state 'horizontal shift' consistent with a decrease in fictive temperature [41].

4. Discussion and conclusion

Comparing the dynamic shear modulus and the dielectric permittivity in the linear response limit for tetramethyl-tetraphenyl-trisiloxane, a common temperature-dependence of the timescale of structural relaxation becomes evident. The two timescales differ by a positive factor that is constant over the presented temperature range, a behavior that suggests that both quantities, shear modulus and dielectric permittivity, are governed by the same underlying process, namely the process of structural relaxation. The coupling of the timescales of these two quantities as well as the positive constant factor connecting the two timescales is observed for various molecular glass-formers. The type of inter-molecular interactions does not seem to influence this behavior, while secondary processes affect it strongly resulting in an apparent decoupling of timescales. This effect of secondary or β processes is based on their temperature dependence, $\tau_\beta(T)$, departing significantly from that of the primary or α process.

Mechanical experiments can easily be conducted within the nonlinear response regime, which is marked by the increase in mechanical compliance with increasing intensity of mechanical excitation, signal contributions at higher order frequencies, as well as strongly distorted Lissajous-figures. The mechanically induced softening does not necessarily depend on the type of mechanical excitation and occurs for experiments involving a bias mechanical excitation as well as for oscillatory

experiments with a high harmonic amplitude. The cause for the observed mechanical softening is the activation of STZ's by the mechanical excitation beyond the level of thermally induced rearrangements. The total potential energy barrier for an STZ in metallic glasses can be approximated by

$$W_{\mathrm{STZ}} = \frac{8}{\pi^2}\gamma_{\mathrm{c}}^2 G\Omega\varsigma. \tag{7}$$

with the average shear limit $\gamma_{\mathrm{c}} = 0.027(2)$ based on the cooperative shear model [42], the actual volume of the STZ's plastic core Ω, and a dressing factor ζ based on the confinement of the STZ within the elastically deformed surroundings [35, 36, 43]. With the shear modulus for $Pd_{40}Ni_{40}P_{20}$ of $G = 30$ GPa, and assuming that the actual volume of the STZ is identical to the activation volume V_0, which is approximately 10 nm^3 based on data for Pd-based metallic glass [29], the energy barrier can be determined to $W_{\mathrm{STZ}} \approx 5 \times 10^{-19}$ J. This value is two orders of magnitude above the thermal energy for the presented nonlinear mechanical experiment ($W_{\mathrm{th}} = k_{\mathrm{B}}T = 7.8 \times 10^{-21}$ J). Judged by the present degree of nonlinearity for sufficiently high stress amplitudes and the connection of nonlinearity to mechanical activation of STZ's, one can assume that mechanical energies involved are considerably larger than $k_{\mathrm{B}}T$, as $W_{\mathrm{STZ}} > W_{\mathrm{th}}$.

Can we assume that mechanical and dielectric nonlinear effects are based on the same cause, just as indicated in the linear response limit? In other words, are shear transformations triggered in nonlinear dielectric experiments as well, assuming rigidity of the molecular shape and the dipole moment? Reasoning with the energies involved in nonlinear dielectric experiments suggest that this is not the case. Based on the example of the dielectric response to a harmonic electric field with a large amplitude of $E_0 = 671$ kV cm^{-1} for glycerol [27], the energy based on the molecular dipole moment for glycerol, $\mu = 2.61$ D, amounts to $W_{\mathrm{diel}} = \mu E = 5.8 \times 10^{-22}$ J, which is a factor of 5 below W_{th} ($T = 213$ K). A more realistic estimate involves the effective dipole moment that accounts for correlation effects, either via the Kirkwood correlation factor with $\mu_{\mathrm{eff}} = \mu\sqrt{g_{\mathrm{K}}}$ [39], or via glassy correlations $\mu_{\mathrm{eff}} = \mu\sqrt{N_{\mathrm{corr}}}$ [44]. While correlations may bring W_{diel} up a factor of 10, it remains that even the highest experimentally achievable dielectric energies are far below W_{STZ}, assuming that a similar reasoning for mechanical energies can be applied for molecular glass-formers as was presented for metallic glasses. Note that the application of high electric fields such that $W_{\mathrm{diel}} > W_{\mathrm{th}}$ is prohibited by dielectric breakdown, i.e., sample failure, for practically all dielectric materials. Another indication that dielectric nonlinear effects have a different origin than mechanical ones is found in the apparent change of fictive temperature: while large amplitudes of harmonic electric fields result in a shift of parts of the relaxation mode spectrum towards higher frequencies, consistent with an increase in fictive temperature ($T_{\mathrm{f}} > T$), large electric bias fields are connected to an apparent decrease in fictive temperature ($T_{\mathrm{f}} < T$).

While the dielectric and mechanical response of experiments within the linear limit reflect different aspects of the same underlying process which is the structural relaxation of the material, nonlinear effects in dielectric and mechanical experiments do not share a common cause. While mechanical experiments involve energies that are high enough to trigger shear transformations within the material and thus clearly exceed the thermal energy $k_{\mathrm{B}}T$, dielectric energies are clearly below that limit, so that $W_{\mathrm{diel}} \ll W_{\mathrm{STZ}}$ and the athermal activation of correlated microscopic rearrangements due to the applied electric field cannot be expected. As a consequence of the very different natures of the mechanical and dielectric nonlinear behavior, the two response functions may differ even if the temperature and the fictive temperature are the same.

Acknowledgments

BR is grateful for support from the VILLUM Foundation's Matter Grant (No. 16515).

ORCID iDs

Birte Riechers https://orcid.org/0000-0003-4437-9844
Ranko Richert https://orcid.org/0000-0001-8503-3175

References

[1] Ediger M D, Angell C A and Nagel S R 1996 *J. Phys. Chem.* **100** 13200
[2] Angell C A, Ngai K L, McKenna G B, McMillan P F and Martin S W 2000 *J. Appl. Phys.* **88** 3113
[3] Swallen S F, Kearns K L, Mapes M K, Kim Y S, McMahon R J, Ediger M D, Wu T, Yu L and Satija S 2007 *Science* **315** 353
[4] Berne B J and Pekora R 1976 *Dynamic Light Scattering* (New York: Wiley)
[5] Richert R 2014 *Adv. Chem. Phys.* **156** 101
[6] Timoshenko S P and Goodier J N 1970 *Theory of Elasticity* (New York: McGraw Hill)
[7] Böhmer R, Diezemann G, Hinze G and Rössler E 2001 *Prog. Nucl. Magn. Reson. Spectrosc.* **39** 191
[8] Zheng Q, Zhang Y, Montazerian M, Gulbiten O, Mauro J C, Zanotto E D and Yue Y 2019 *Chem. Rev.* **119** 784
[9] Vogel H 1921 *Phys. Z.* **22** 645
[10] Fulcher G S 1925 *J. Am. Ceram. Soc.* **8** 339
[11] Tammann G and Hesse W 1926 *Z. Anorg. Allg. Chem.* **156** 245
[12] Kubo R 1966 *Rep. Prog. Phys.* **29** 255
[13] Gardon R and Narayanaswamy O S 1970 *J. Am. Ceram. Soc.* **53** 380
[14] Christensen T and Olsen N B 1995 *Rev. Sci. Instrum.* **66** 5019
[15] Igarashi B, Christensen T, Larsen E H, Olsen N B, Pedersen I H, Rasmussen T and Dyre J C 2008 *Rev. Sci. Instrum.* **79** 045105
[16] Jakobsen B, Niss K and Olsen N B 2005 *J. Chem. Phys.* **123** 234511
[17] Schröter K, Wilde G, Willnecker R, Weiss M, Samwer K and Donth E 1998 *Eur. Phys. J.* B **5** 1
[18] McCrum N G, Read B E and Williams G 1967 *Anelastic and Dielectric Effects in Polymeric Solids* (New York: Dover)
[19] Dyre J C 1991 *J. Non-Cryst. Solids* **135** 219
[20] Jäckle J and Richert R 2008 *Phys. Rev.* E **77** 031201
[21] Jakobsen B, Hecksher T, Christensen T, Olsen N B, Dyre J C and Niss K 2012 *J. Chem. Phys.* **136** 081102
[22] Jakobsen B, Niss K, Maggi C, Olsen N B, Christensen T and Dyre J C 2011 *J. Non-Cryst. Solids* **357** 267
[23] Richert R 2017 *J. Phys.: Condens. Matter* **29** 363001
[24] Finkhäuser S 2017 Mechanische spektroskopie an PMMA-systemen: nichtlineares verhalten und UV-aktive

blockcopolymere *PhD Thesis* Georg-August-Universität Göttingen
[25] Riechers B and Samwer K 2017 *Eur. Phys. J. Spec. Top.* **226** 2997
[26] Richert R and Weinstein S 2006 *Phys. Rev. Lett.* **97** 014201
[27] Bauer T, Lunkenheimer P, Kastner S and Loidl A 2013 *Phys. Rev. Lett.* **110** 107603
[28] Herrero-Gómez C and Samwer K 2018 *J. Phys.: Condens. Matter* **30** 46
[29] Schwabe M, Küchemann S, Wagner H and Samwer K D 2011 *J. Non-Cryst. Solids* **357** 490
[30] Hyun K, Wilhelm M, Klein C O, Cho K S, Nam J G, Ahn K H, Lee S J, Ewoldt R H and McKinley G H 2011 *Prog. Polym. Sci.* **36** 1697
[31] Yu H-B, Richert R, Maaß R and Samwer K 2015 *Nat. Commun.* **6** 7179
[32] Adam G and Gibbs J H 1965 *J. Chem. Phys.* **43** 139
[33] Eshelby J D 1957 *Proc. R. Soc.* A **241** 376
[34] Eshelby J D 1959 *Proc. R. Soc.* A **252** 561
[35] Argon A S 1979 *Acta Metall.* **27** 47
[36] Argon A S and Shi L T 1983 *Acta Metall.* **31** 449
[37] Debye P 1929 *Polar Molecules* (New York: Chemical Catalog Company)
[38] Herweg J 1920 *Z. Phys.* **3** 36
[39] Böttcher C J F 1973 *Theory of Electric Polarization* (Amsterdam: Elsevier)
[40] Małecki J 1997 *J. Mol. Struct.* **436–437** 595
[41] Riechers B and Richert R 2018 *Phys. Chem. Chem. Phys.* **21** 32
[42] Johnson W L and Samwer K 2005 *Phys. Rev. Lett.* **95** 195501
[43] Eshelby J D 1961 *Proc. R. Soc.* A **241** 376
[44] Albert S *et al* 2016 *Science* **352** 1308